Optical Lattice Model Toward Nonreciprocal Invisibility Cloaking

Tomohiro Amemiya, *Member, IEEE*, Masato Taki, Toru Kanazawa, *Member, IEEE*, Takuo Hiratani, *Student Member, IEEE*, and Shigehisa Arai, *Fellow, IEEE*

***Abstract*— We propose the design theory of nonreciprocal invisibility cloaking for an optical camouflage device with unidirectional transparency in which a person in the cloak can see the outside but cannot be seen from the outside. Existing theories of designing invisibility cloaks cannot be used for this purpose, because they are based on the transformation optics that uses the Riemannian metric tensor independent of direction. To realize nonreciprocal cloaking, we propose the theory of effective electromagnetic field for photons, which is an extended version of the theory of effective magnetic field for photons. The effective electromagnetic field can be generated using a photonic resonator lattice. The Hamiltonian for a photon in this field has a similar form to that of the Hamiltonian for a charged particle in an electromagnetic field. Incident photons, therefore, experience a Lorentz-like force and a Coulomb-like force and show nonreciprocal movement depending on their traveling direction. We design an actual invisibility cloaking system on the basis of this theory and, with the aid of computer simulation, confirm the nonreciprocal propagation of light needed for nonreciprocal cloaking.**

***Index Terms*— Quantum theory, electromagnetic propagation, optical resonance.**

I. Introduction

THE invisibility cloak is a unique cloaking device that makes its wearer transparent and therefore invisible to others. Magical invisibility cloaks, of course, belong to the world of fairy tales and science fictions. It is physically possible, however, to make a physical object seem invisible if we can cause incident light to avoid the object, flow around it, and then return to its original trajectory undisturbed [1]–[4]. A promising development for such physical invisibility cloaking is the recent progress in the research into metamaterials [6]–[11]. Metamaterials are artificial materials consisting of multiple nanostructural elements such as minute resonators, arranged periodically with a pitch smaller than the wavelength of light. They can exhibit extraordinary permittivity and permeability values that are not found in nature. Using metamaterials enables us to create a unique electromagnetic field surrounding an object we wish to hide, and it should therefore be possible to control the optical path around the object to make it appear invisible.

A method of designing invisibility cloaks was first proposed by Pendry et al. in 2006 and, at about the same time, by Leonhardt [1], [2]. Their methods are based on the theory of transformation optics. According to this theory, a distorted space is equivalent (in terms of the propagation of light) to a flat space filled with a medium having an appropriate spatial distribution of its refractive index. To realize invisibility cloaking, they first designed a hypothetical distorted space in which light was bent away from the object that they wished to hide. They then imitated the distorted space in the real flat space, by surrounding the object with a metamaterial that had an appropriate refractive-index distribution determined from analysis of the Riemannian metric tensor of the distorted space. Their idea attracted the attention of many researchers and much effort has since been expended to develop metamaterials for use in invisibility cloaking, with many reports of cloaking experiments being conducted [12]–[17].

An invisibility cloak designed using transformation optics has a closed region, called a cloaked region, which incident light from every directon 'avoids'. A person hiding in the cloaked region therefore seems invisible to external onlookers. However, a serious, critical problem occurs here. That is, no light can enter the cloaked region, and consequently the person hiding therein will not be able to see outside. This greatly reduces the usefulness of invisibility cloaks. A practical invisibility cloak must have unidirectional transparency such that a person inside cannot be seen from the outside but can see the outside (see Fig. 1). However, the transformation optics cannot be applied to such nonreciprocal cloaking because it uses the Riemannian metric tensor independent of direction [1], [2].

To overcome this problem, we have formulated a theory of nonreciprocal cloaking that can achieve unidirectional transparency. Our theory has no relation to transformation optics but is instead based on 'the theory of an effective magnetic field for photons' proposed in Refs. [18] and [19]. We have extended their theory to add the concept of an 'effective electric field for photons.' This effective electromagnetic field can be generated using a photonic resonator lattice,

Manuscript received September 1, 2014; revised December 6, 2014; accepted January 3, 2015. Date of publication January 8, 2015; date of current version January 30, 2015. This work was supported by the Japan Society for the Promotion of Science through the Grants-in-Aid for Scientific Research within the Ministry of Education, Culture, Sports, Science, and Technology under Grant 24246061, Grant 25420321, and Grant 25420322.

T. Amemiya and S. Arai are with the Quantum Nanoelectronics Research Center, Tokyo Institute of Technology, Tokyo 152-8550, Japan (e-mail: amemiya.t.ab@m.titech.ac.jp; arai@pe.titech.ac.jp).

M. Taki is with the RIKEN Nishina Center for Accelerator-based Science, Wako 351-0198, Japan (e-mail: taki@riken.jp).

T. Kanazawa is with Department of Physical Electronics, Tokyo Institute of Technology, Tokyo 152-8552, Japan (e-mail: kanazawa.t.aa@m.titech.ac.jp).

T. Hiratani is with Department of Electrical and Electronic Engineering, Tokyo Institute of Technology, Tokyo 152-8552, Japan (e-mail: hiratani.t.aa@m.titech.ac.jp).

Color versions of one or more of the figures in this paper are available online at http://ieeexplore.ieee.org.

Digital Object Identifier 10.1109/JQE.2015.2389853

0018-9197 © 2015 IEEE. Personal use is permitted, but republication/redistribution requires IEEE permission.
See http://www.ieee.org/publications_standards/publications/rights/index.html for more information.

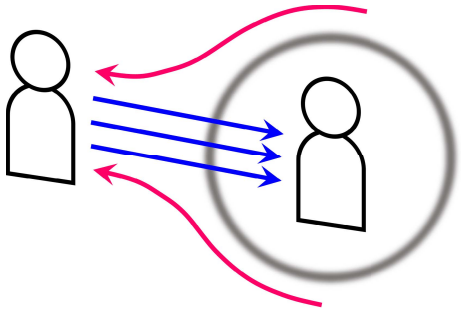

Fig. 1. Concept of *nonreciprocal* cloaking. Light traveling rightward proceeds undisturbed (blue line). The person in the cloaked region can therefore see the left-hand side. Light traveling leftward circumvents the cloaked region (red curve). The person in the cloaked region therefore seems invisible from the left-hand side.

which is a kind of metamaterial (or photonic crystal). Using this field, we can direct light to demonstrate the nonreciprocal movement required for nonreciprocal invisibility cloaking. On the basis of our theory, we propose a method of designing nonreciprocal cloaking devices.

In the following sections, we first explain the concept of the effective electromagnetic field for photons produced by a photonc resonator lattice (section 2). Then, we explain the procedure of designing nonreciprocal invisibility cloaks (section 3). The nonreciprocal movement of photons under an effective electromagnetic field is visualized with the aid of Schrödinger-equation simulation (section 4). We design an actual cloaking system and confirm its nonreciprocity by simulation (section 5). Section 6 summarizes our results.

II. Effective Electromagnetic Field for Photons

As regards background knowledge, we need to familiarize ourselves with the theory of the *'effective magnetic field for photons'* (see [18]–[21] for related discussion). The core principle of this theory is that a specific photonic resonator lattice, a kind of metamaterial, can generate a virtual field for photons that is analogous to a magnetic field for moving charged particles. The concept of the effective magnetic field (EfM) provides important impetus for the development of nonreciprocal invisibility cloaking. Using the EfM, we can break time-reversal symmetry in optics and give a certain extent of nonreciprocity to the propagation of light. However, nonreciprocal cloaking needs an even higher nonreciprocity in the light propagation. For example, as will be shown in section 3, forward-propagating light must avoid and circumvent the cloaked region, whereas backward-propagating light must travel in a straight line to enter the cloaked region. Such a high nonreciprocity cannot be obtained using the EfM alone.

To overcome this problem, we propose the introduction of a second field acting upon the photons, analogous to an electric field for charged particles. Let us call this field an *'effective electric field'*. Using the effective electric field (EfE) in addition to the EfM, we will be able to control the path of the incident light with high nonreciprocity.

Consider a lattice (see Fig. 2) consisting of two kinds of alternately arrayed photonic resonators, A and B. Figure 2 shows a two-dimensional square lattice, but this discussion can also be applied to a three-dimensional lattice with the sodium chloride structure. Let us assume that each resonator is dynamically coupled to its nearest neighbors, and that the coupling strength is modulated harmonically. The resonance frequency of each resonator is not constant but depends on its position. We express the resonance frequency as $\omega_A(i) = \omega_A + V_A\varphi_i$ for resonator A, and $\omega_B(j) = \omega_B + V_B\varphi_j$ for resonator B, where V_A and V_B are frequency parameters and φ_i and φ_j are dimensionless parameters assigned to the resonators at positions i and j, respectively. From the tight-binding model and second quantization, the Hamiltonian for a photon can be given by

$$H = \sum_i \left(\hbar\omega_{\mathrm{A}} + V_A\varphi_i\right) a_i^\dagger a_i + \sum_j \left(\hbar\omega_{\mathrm{B}} + V_B\varphi_j\right) b_j^\dagger b_j + V \sum_{<i,j>} \cos\left(\Omega t + \phi_{ij}\right)\left(a_i^\dagger b_j + b_j^\dagger a_i\right), \quad (1)$$

where subscripts i and j indicate the position of resonators A and B on the lattice system, V is the coupling strength to the nearest neighbors, $\Omega/\hbar$ is the frequency of the coupling modulation, ϕ_{ij} is the modulation phase for two adjacent resonators at positions i and j, a_i^+ and a_i are creation and annihilation operators in resonator A, and b_j^+ and b_j are creation and annihilation operators in resonator B. The vacuum state, $0\rangle$, is therefore annihilated by a_i and b_j. This Hamiltonian consists of the free-field component (composed of two types of harmonic oscillators with frequencies ω_A and ω_B)

$$H_0 = \sum_i \hbar\omega_{\mathrm{A}} a_i^\dagger a_i + \sum_j \hbar\omega_{\mathrm{B}} b_j^\dagger b_j, \quad (2)$$

and the interaction component, whose coupling is controlled by V. Let us move the visualization of this quantum system from the Schrödinger expression to that of the interaction. The interaction setup is a hybrid of the Schrödinger and Heisenberg visualizations, and the time evolution of an operator is given by the free Hamiltonian, H_0, while the evolution of a state is expressed by changes in the interaction Hamiltonian, H_I. The creation and annihilation operators in the interaction setup are therefore

$$c_i(t) \equiv e^{\frac{itH_0}{\hbar}} a_i e^{-\frac{itH_0}{\hbar}} = e^{-\frac{it\omega_A}{\hbar}} a_i, \quad (3)$$

$$c_j(t) \equiv e^{\frac{itH_0}{\hbar}} b_j e^{-\frac{itH_0}{\hbar}} = e^{-\frac{it\omega_B}{\hbar}} b_j \quad (4)$$

and the interaction Hamiltonian, H_I, is

$$H_I = e^{\frac{itH_0}{\hbar}}\left(H - H_0\right)e^{-\frac{itH_0}{\hbar}} = V \sum_{<i,j>} \cos\left(\Omega t + \varphi_{ij}\right)\left(c_i^\dagger(t)\, c_j(t) + c_j^\dagger(t)\, c_i(t)\right) + \sum_i V_A\varphi_i c_i^\dagger c_i + \sum_j V_B\varphi_j c_j^\dagger c_j. \quad (5)$$

Let us assume $\hbar\Omega = \omega_A - \omega_B$ for simplicity. Using the interaction picture and rotational wave approximation,

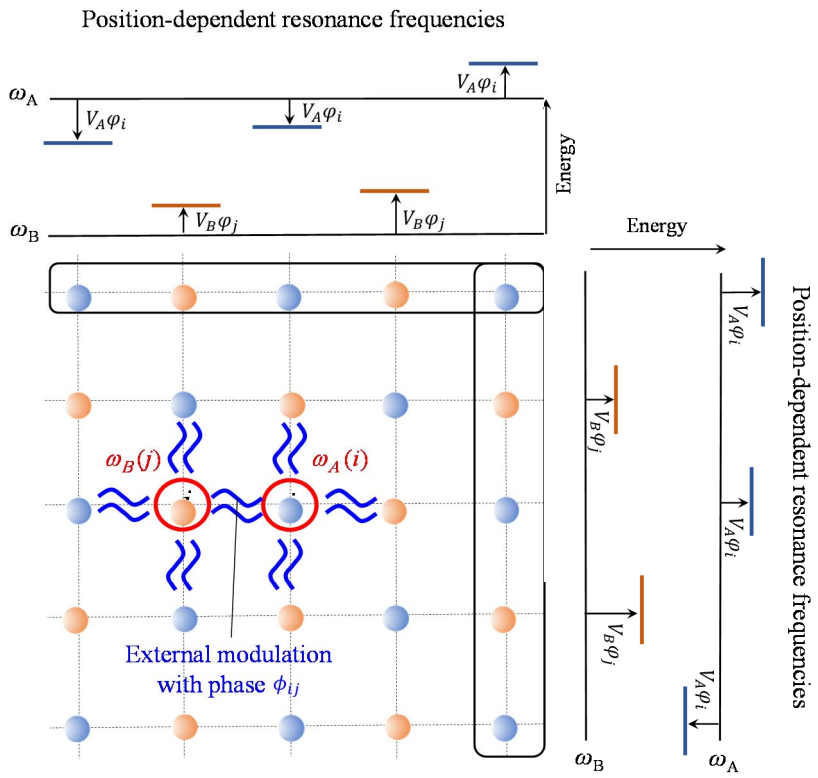

Fig. 2. Optical lattice for generating an electromagnetic field for photons. The resonance frequency (ω_A and ω_B) of each resonator depends on resonator position (i and j). Each resonator is dynamically coupled to its nearest neighbors, with the coupling strength modulated harmonically. The modulation phase for each resonator pair is ϕij.

the Hamiltonian simplifies to give

$$H_I \cong H_{eff} = \frac{V}{2}\sum_{<i,j>}\left(e^{-i\phi_{ij}}c_i^\dagger c_j + e^{i\phi_{ij}}c_j^\dagger c_i\right) + \sum_i V_A\varphi_i c_i^\dagger c_i + \sum_j V_B\varphi_j c_j^\dagger c_j, \quad (6)$$

and this approximation therefore drops the time-dependent vibration terms, $e^{\pm 2i\Omega t}$. This Hamiltonian consists of the time-independent creation/annihilation operators

$$c_i \equiv c_i\,(t=0)\,, \quad c_j \equiv c_j\,(t=0), \quad (7)$$

and the coefficients are also time-independent.

The point here is that Eq. 6 has the same form as that of the tight-binding Hamiltonian for a charged particle in an electromagnetic background field [22]. This means that the photonic resonator lattice shown in Fig. 2 introduces an electromagnetic-like field to the photons.

The first term on the right-hand side of Eq. 6 corresponds to the motion of a photon under the influence of the EfM. Net phase difference $\Sigma\phi ij$ that is applied to each loop in the lattice produces an Aharanov-Bohm-like phase shift of the wavefunction of photons in the lattice. This means that a magnetic-like field (i.e. EfM) penetrating the loop is produced by $\Sigma\phi ij$. Therefore photon motion in this system is not symmetric for time reversal, which is similar to the motion of electrons traveling in an external magnetic field. The magnitude and direction of the EfM can be controlled by adjusting the spatial distribution of the coupling strength, V, and the modulation phase difference, ϕ_{ij}. A photon affected by the EfM experiences a 'Lorentz-like' force as if it were a charged particle in a magnetic field [23].

The second and third terms describe the motion induced by an electric-like field (i.e. EfE). The magnitude and direction of the EfE can also be controlled by adjusting the spatial distribution of the resonance frequency, $V_{A(B)}\varphi_{i(j)}$. A photon under the influence of the EfE experiences a 'Coulomb-like' force as if it were a charged particle in an electric field.

III. Nonreciprocal Invisibility Cloaking Using Effective Electric and Magnetic Fields

Using a simple example, we illustrate the design approach for nonreciprocal invisibility cloaks that make use of the EfE an EfM. The design procedure is as follows:

A. Step 1: Designing the Directed Optical Path for Nonreciprocal Cloaking

The first stage is the creation of a directed optical path diagram for nonreciprocal cloaking. For example, let us consider a cloaking device that functions in such a manner that its wearer, when looking toward observers, can see them but is not visible to them. To be more precise, consider a specific cloaking device such that: (i) the device has a closed cloaked region with forward-backward directionality and its wearer angles the forward direction toward the observers, (ii) the wearer can see the observers clearly, whereas the observers

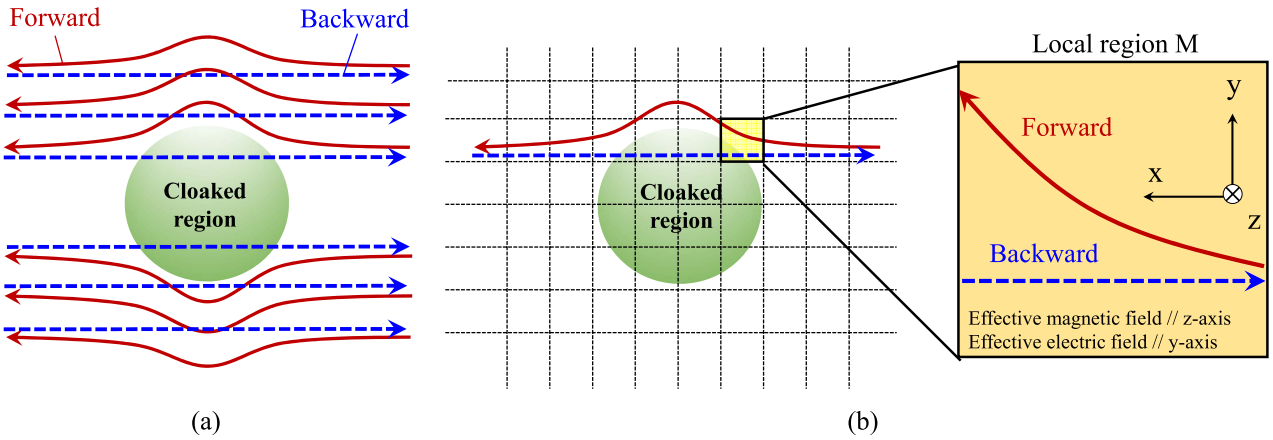

Fig. 3. Ray trajectory for nonreciprocal cloaking. (a) Optical path for forward/backward direction. (b) Directing light to follow the designated optical path. We divide the space surrounding the cloaking region into small local spaces and control the movement of the light (or photons) in each local space. The entire cloaking device can be built by locating a photonic resonator lattice in every local space and adjusting the parameters of each lattice as necessary.

can see only the background behind the wearer and cannot see the wearer himself.

For such unidirectional transparency, the device must redirect incident light along different paths depending on the original direction of the light. Figure 3a shows the required directed optical path on a plane passing through the optical axis of the system. In this figure, the forward direction of the device is set right-to-left and the observers are on the left-hand side of the device. The cloaking effect requires directional propagation of light such that:

(a) forward-traveling light (red arrows in Fig. 3a) circumvents the cloaked region and returns undisturbed to its original trajectory so that a person in the cloaked region will seem invisible to the observers on the left;

(b) backward-traveling light (blue arrows in Fig. 3(a)) proceeds undisturbed so that the person in the cloaked region can see the observers on the left.

B. Step 2: Directing Light to Follow the Required Optical Path

Next, we divide the space surrounding the cloaked region into small local spaces and consider the movement of light (or photons) in each local space. As an example, let us take a local space (denoted by the yellowish square in Fig. 3b). In this space, forward-traveling photons (red arrows) must be deflected upward, whereas backward-traveling photons (blue arrows) must continue to move in a straight line with no deflection. If the traveling particles were electrons, such motion could be achieved by the application of a magnetic field in the z-direction and an electric field in the y-direction, each with an appropriate magnitude. For photons, the same motion can be achieved through the use of a z-directed EfM and a y-directed EfE instead of a magnetic and an electric field. To achieve this, we locate a photonic resonator lattice in the local space and set appropriate lattice parameters so that the photons will follow the directed optical path shown in Fig. 3(b).

To generate a uniform z-directed EfM and a uniform y-directed EfE with a resonator lattice, we set the parameters ϕ_{ij} and $\varphi_{i(j)}$ of the lattice as follows (see Fig. 4):

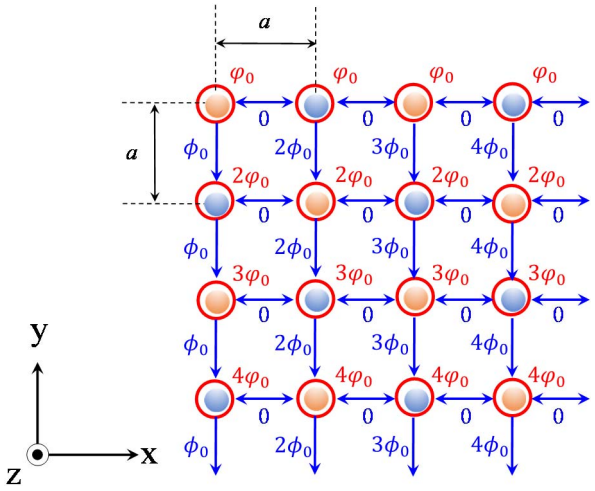

Fig. 4. Spatial distributions of modulation phase difference ϕ_{ij} and resonance frequency $\varphi_{i(j)}$ to generate uniform z-directed EfM and uniform y-directed EfE.

1. Parameter ϕ_{ij} is:
   - (1-1) proportional to the column index and increases by ϕ_0 for one index step;
   - (1-2) equal between the vertical couplings on the same column;
   - (1-3) 0 on the horizontal couplings.
2. Parameter $\varphi_{i(j)}$ is:
   - (2-1) proportional to the row index and increases by φ_0 for one index step;
   - (2-2) equal between the resonators on the same row.

The lattice constant, a, is set sufficiently smaller than the dimensions of the local spaces. For simplicity, we assume $V_A = V_B$ here. Under these conditions, the magnitude, B_{eff}, of the z-directed EfM is given by

$$B_{eff} = \frac{1}{a^2} \oint A\left(\vec{X}\right) \cdot d\vec{X}, \tag{8}$$

where

$$\frac{2\pi}{\Phi_0}\int_{\vec{X}_i}^{\vec{X}_j} A\left(\vec{X}\right)\cdot d\vec{X} = \phi_{ij}, \tag{9}$$

with $\mathrm{A}\left(\vec{X}\right)$ the effective photon gauge potential and $\Phi_0 = hc/e$ the quantum unit of the magnetic flux. On the other hand, the magnitude, E_{eff}, of the y-directed EfE is given by

$$E_{eff} = -\frac{\phi\left(\vec{X}_k\right) - \varphi\left(\vec{X}_l\right)}{a}, \tag{10}$$

and

$$\varphi\left(\vec{X}_{k(l)}\right) = \frac{\hbar^2 V_A}{mea^2 V}\varphi_{k(l)}, \tag{11}$$

where k and l are two adjoining lattice points and $\varphi\left(\vec{X}\right)$ is the effective scalar potential for the EfE.

Under these EfM and EfE, a photon will behave as if it were an electron under the influence of magnetic and electric fields with magnitudes B_{eff} and E_{eff}. The nonreciprocal movement of the photons is visualized in section 4.

C. Step 3: Equipping the Cloaked Region With Many Resonator Lattices

The entire cloaking device can be built by locating a photonic resonator lattice in every local space and adjusting the parameters of each lattice so that the local optical paths are connected into the overall optical path shown in Figs. 3a and 3b. By surrounding the cloaking region with many resonator lattices with appropriate parameter values, we can create an appropriate spatial distribution of the EfE and EfM around the cloaked region, thereby controlling the movement of the photons and achieving nonreciprocal cloaking.

IV. Visualizing the Nonreciprocal Movement of Photons—Schrödinger Equation Simulation

Appropriate parameter values for each resonator lattice can be determined with the aid of numerical simulation. The lattice has several parameters, including ϕ_0 and φ_0, and in this study we find their optimal values simply through an exhaustive search technique, though a more efficient approach may exist.

To observe the forward and backward movement of photons in a given local space, we placed a photon in the center of the local space and simulated its subsequent motion. In our simulation, we used the Hamiltonian given by Eq. 1 with the initial state of the photon expressed by the Gaussian wave packet such that

$$\left|\psi\left(0\right)\right\rangle = C\sum_{m,n} e^{-\frac{\sigma}{2}(m-m_0)^2-\frac{\sigma}{2}(n-n_0)^2} e^{ikm} a^{\dagger}_{(m,n)}\left|0\right\rangle, \tag{12}$$

where C is the normalization factor, σ is the characteristic width, the point (m_0, n_0) represents the central position at time $= 0$, and k is the wavenumber of the photon (positive k is for forward displacement and negative k indicates backward displacement). The time development of the photon state is expressed as

$$\left|\psi\left(t\right)\right\rangle = e^{-iHt}\left|\psi\left(0\right)\right\rangle, \tag{13}$$

where t is time. The distribution and the central position of the wavefunction changes as the wave propagates, and the motion of the central position corresponds to the trajectory of the photon. To solve Eq. 13, we used the 8th-degree Taylor series approximation of e^{-iHt} around $t = 0$.

Figure 5 shows the result of the simulation, an example of the time development of the photon wavefunction for forward and backward displacement, simulated using the lattice parameters: $\phi_0 = 0.3$, $\varphi_0 = 0.3$, $V_A = V_B = 3$, and $V = 0$, 2. A movement to the left side shows forward propagation, and

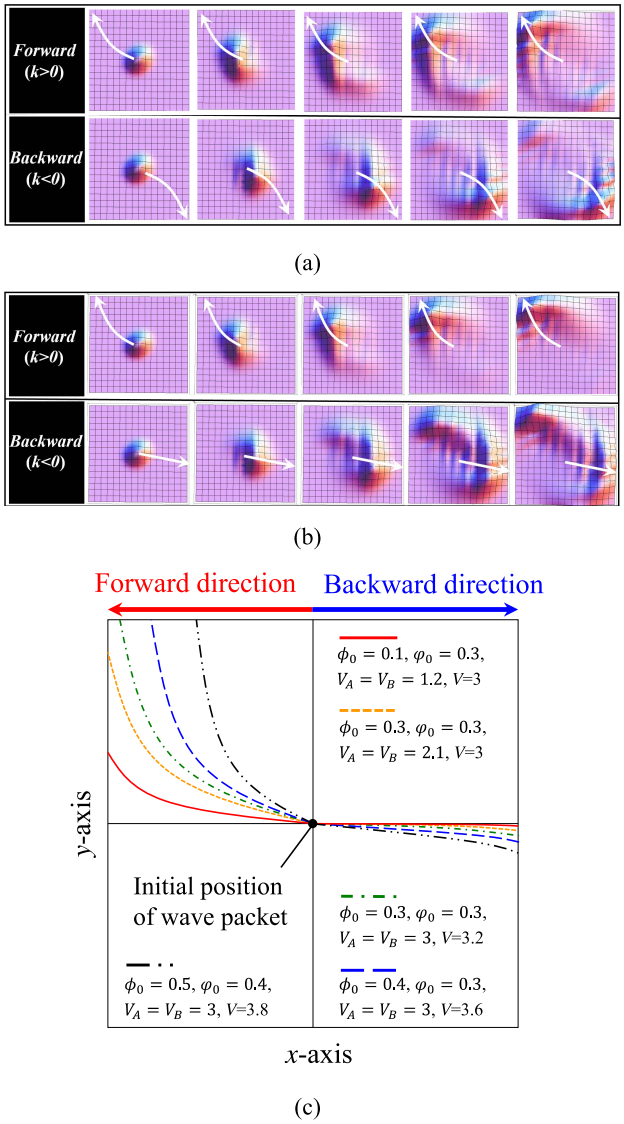

Fig. 5. Time development of photon wavefunction for forward and backward propagation; (a) snapshots for 5 time steps under the influence of an EfM only, a photon experiences a Lorentz-like force and draws a simple circular trajectory (white arrows); (b) under the influence of an EfE in addition to an EfM, a photon shows nonreciprocal motion (white arrows). The parameters used for simulation are (a) $\phi_0 = 0.3$, $\varphi_0 = 0.3$, $V_A = V_B = 3$, $V = 0$ and (b) $\phi_0 = 0.3$, $\varphi_0 = 0.3$, $V_A = V_B = 3$, $V = 2$; (c) nonreciprocal movement of photon for various parameter sets.

a movement to the right side shows backward propagation. Figure 5a shows the development with an EfM alone ($V_A = V_B = 3$, $V = 0$) while Fig. 5b corresponds to the presence of both an EfM and an EfE ($V_A = V_B = 3$, $V = 2$). Both figures show forward and backward propagation (snapshots for 5 time steps) and the distribution of the wave packet in the lattice is visualized using color amplitude imaging. The central position of the wave packet changes as the wave propagates and its movement corresponds to the trajectory of the photon (indicated by white arrows). Under the influence of an EfM only, a photon experiences a Lorentz-like force and completes a simple circular displacement. The trajectory of a forward propagating photon and that of a reverse propagating photon are in 2-fold rotational symmetry with each other. This cannot produce nonreciprocal cloaking. In contrast, under the influence of an EfE in addition to an EfM, the symmetry is broken. For a forward propagating photon, the Coulomb-like force is added to the Lorentz-like force, so the travelling photon is deflected strongly. For a backward propagating photon, the Coulomb-like force cancels the Lorentz-like force, and the photon proceeds undisturbed.

Figure 5c shows the non-reciprocal movement of a photon (the center of a photon wave packet) for various parameter values. By adjusting parameters, we can control a photon so that it will draw an appropriately curved trajectory in forward traveling and maintain its linear motion in backward traveling. Therefore, we can achieve nonreciprocal cloaking by setting appropriate parameter values for every local space in Fig. 3b.

V. Proposal for Experimental Implementation

In this section, we discuss the experimental implementation of our resonator lattice. For the EfM resonator lattice, a sophisticated method of implementation have been proposed [18], [19]. Using this method as a basis, we consider the implementation of our EfM-EfE resonator lattice.

To control the path of the incident light, our resonator lattice first converts the incident light energy to that of lattice vibration and then redirects the flow of the vibrational energy to achieve nonreciprocal cloaking. It is important to transfer the total energy from the light to the lattice, and high-Q resonators are therefore needed for efficient transfer. A suitable resonator element would be a metal LC resonator for the microwave and terahertz regions, and a photonic crystal resonator for the optical regions. We now discuss the latter case.

In our resonator lattice, each resonator element has a different resonant frequency depending on its position and therefore does not resonate with the incident light. This obstructs the efficient energy transfer from the light to the lattice. (In microwave regions, energy transfer through forced oscillation without resonance would be practical, but it is impractical in optical regions because of large energy dissipation.)

The solution is to surround the resonator lattice consisting of buffering resonators with resonance frequencies equal to the incident light frequency. The buffering resonators are set so that they will be coupled with the resonator lattice. With this, the energy of the incident light can be transferred efficiently to the resonator lattice. To suppress slight but inevitable energy dissipation, we consider using resonator cells based on the cavity optomechanical system [24]–[26]. In this system, cavity photons interact with micromechanical resonators and thereby gain energy through the interacion with phonons [27].

TABLE I
Parameters Used in the Simulation

Material & structural parameters		
Parameter	Symbol	Value
Refractive index of pillar	n	3.0
Young's modulus	E	85×10^9 (Pa)
Poisson's ratio	ν	0.3
coefficient of thermal expansion	α	5.7×10^{-6} (Pa)
Density	ρ	5300 (kg/m^3)
Radius of circle pillar for all region	—	$0.2a$
Radius of center circle pillar for optomechanical resonator	—	$0.12a$
Size of rectangle center pillar for dual mode resonator	—	$0.66a \times 0.62a$
Radius of center circle pillar for single mode resonator	—	$0.56a$
Width of a parallel-connected pillar	—	$0.05a$

Figure 6 shows a sample lattice resonator unit consisting of two optical cavities (resonance frequencies: ω_{A} and ω_{B}) and two mechanical resonators (resonance frequency Ω_{m}). As shown in Fig. 6a, incident light with frequency ω_0 absorbs phonon energy and becomes a cavity photon. The system then changes its state to the 'lattice oscillation mode' through the weak retardation regime process. The operation of this system is irreversible and, once the lattice oscillation mode is established, the cavity photons no longer interact with the mechanical oscillators.

Assuming that the lattice has a periodic pillar structure, we confirmed the operation of the lattice unit with the aid of FDTD simulation. We assumed the mechanical resonator consisting of parallel-connected pillars and designed the system so that the maximum optical oscillation and mechanical vibration points would coincide with each other. We calculated the distribution of electromagnetic field and mechanical vibration displacement in the resonator unit. Figure 6b shows the result for basic-mode electromagnetic and mechanical oscillations. Parameters we used are summarized in Table I.

To confirm the successful operation of the device, we compared the values of the leak rate ($\kappa/2\pi$) of cavity photons and the frequency ($\Omega_m/2\pi$) of mechanical oscillation. The calculated Q factor of the optical cavity is about 2640, corresponding to a leak rate of 75 GHz. The oscillation frequency Ω_m and Q factor of the mechanical resonator are 27.5 MHz and 2250. Therefore photon lifetime is far longer than phonon lifetime, and therefore a cavity photon can successfully interact with phonon of the mechanical oscillation to change its energy. Because $\kappa \gg \Omega_m$, the weak retardation regime shown in Fig. 6a is established.

Dynamic coupling between adjacent lattice resonator units can be achieved by inserting an intermediate resonator between

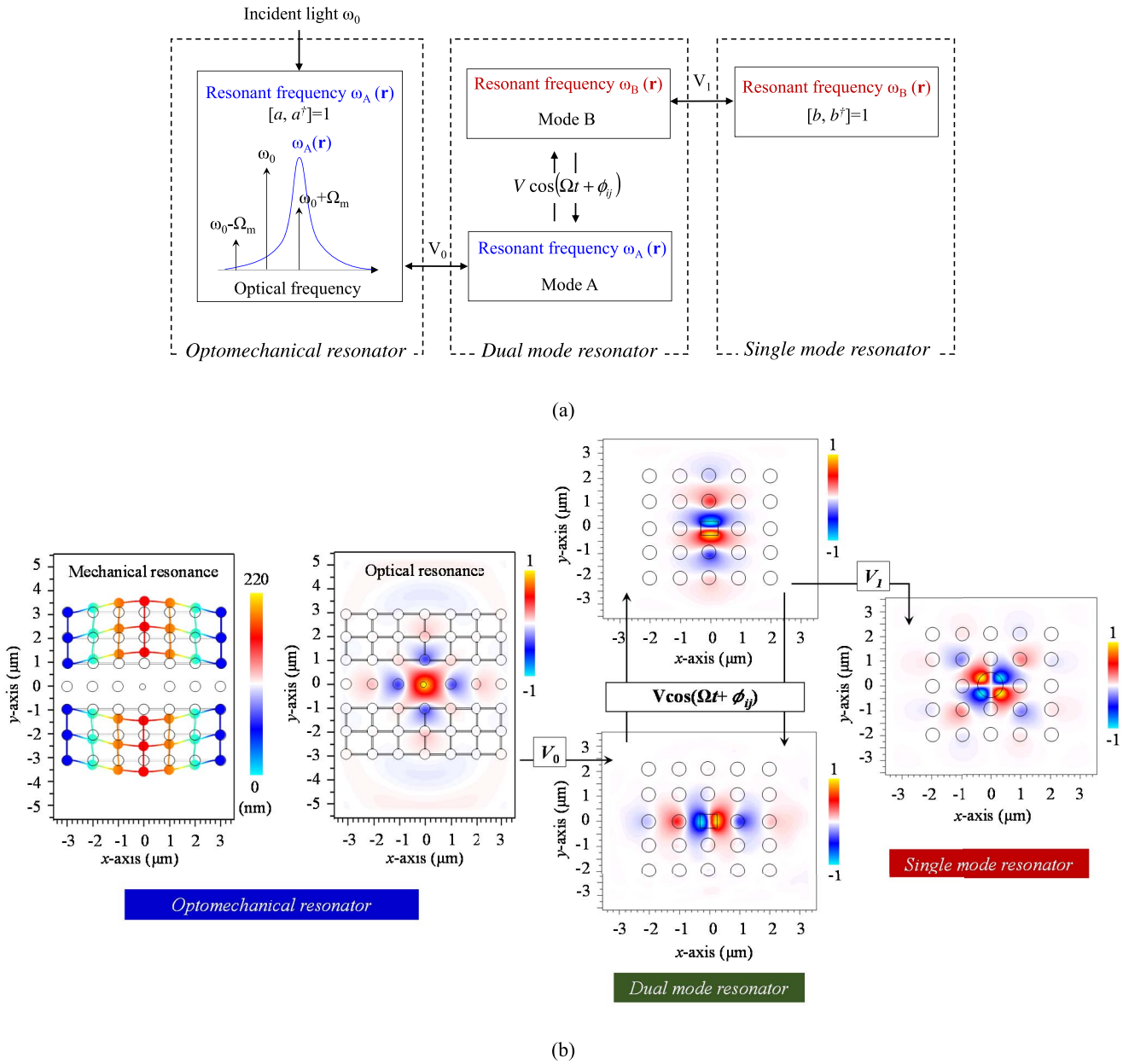

Fig. 6. Operation of resonator cell for nonreciprocal cloaking devices: (a) weak retardation regime process; (b) electric-field distribution in resonator cell simulated with FDTD method (the leftmost shows the displacement distribution of mechanical oscillation). Parameters used in simulation are summarized in Table I.

each pair of adjacent resonator units. The intermediate resonator has two operating conditions, the p_x and p_y modes, with a resonance frequency of ω_A for the p_x mode and ω_B for the p_y mode [28]. It couples with the left resonator, ω_A, in the p_x mode and with the right resonator, ω_B, in the p_y mode. Its operating mode can be switched using an external signal with frequency Ω. In this way, we can achieve dynamical coupling between two adjacent resonators.

We designed a sample cloaking system and simulated its nonreciprocal operation (see Fig. 7). The system consists of the resonator cells arrayed around a region to cloak. As shown in Figs. 7a and 7b, we divided the space around the cloaked region D into 8 regions (A, B, B′, C, C′, B, B′, A) and set an appropriate lattice-parameter values for each region (see the left in Fig. 7(c)). Regions A are buffering regions to receive the energy of incident light. Regions B-B′-C-C′ are core regions to achieve nonreciprocal propagation of light. Figures 7a and 7b also show the photon movement (or optical path) simulated for forward (right-to-left) and backward (left-to-right) propagations. Figure 7c lists the parameters used, and Fig. 7d shows part of the resonator lattice. As expected, forward photons circumvent the cloaked region and travel its exterior (Fig. 7a), whereas backward photons enter and pass through the cloaked region (Fig. 7b). Therefore, nonreciprocal cloaking is successfully performed. In this example, the trajectory of backward

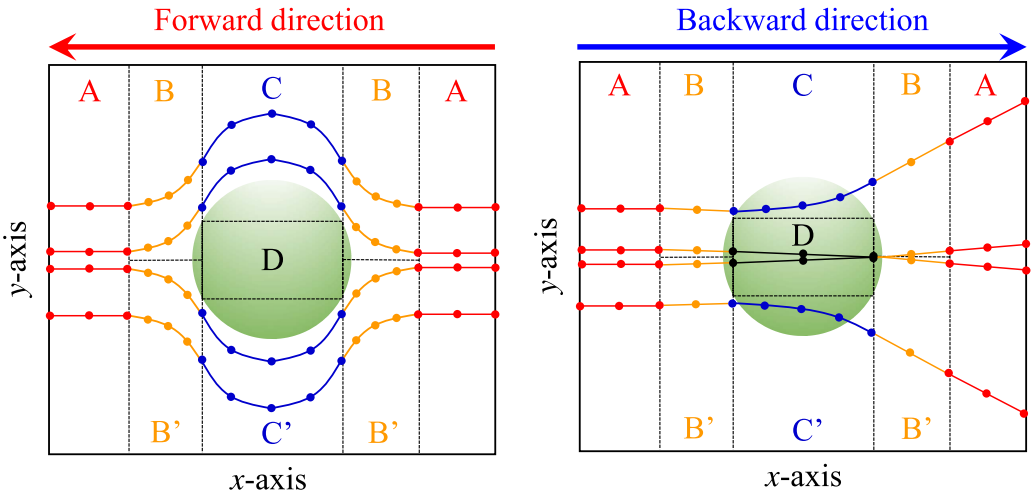

(a) (b)

Simulation parameters

Parameter	Symbol	Value
Interaction between a resonator A and a dual mode resonator	V_0	Variable
Interaction between a dual mode resonator and a resonator B	V_1	Variable
		†We designed resonators to obtain following values.
Parameters for region A (number of x-axis lattice: 20)	—	$\phi_0 = 0, \varphi_0 = 0,$ $V_A = V_B = 0, \omega_0 = \omega_A$
Parameters for region B (B') (number of x-axis lattice: 20)	—	$\phi_0 = 0.3, \varphi_0 = 0.3,$ $V_A = V_B = 1.7, V = 3$ (B' is a reverse field of B)
Parameters for region C (C') (number of x-axis lattice: 40)	—	$\phi_0 = -0.4, \varphi_0 = -0.4,$ $V_A = V_B = 3.6, V = 3$ (C' is a reverse field of C)

(c)

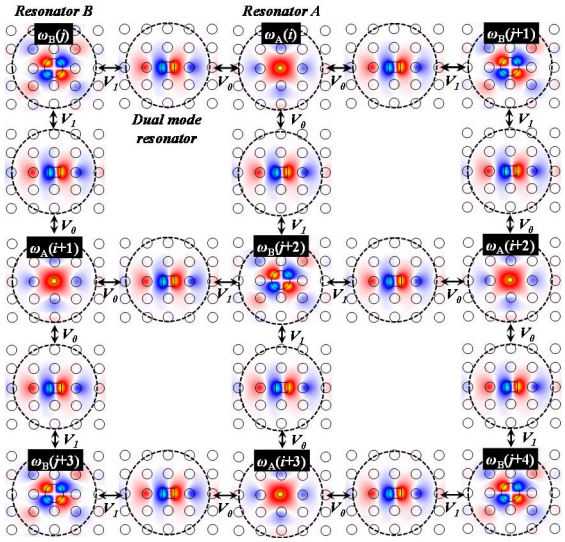

(d)

Fig. 7. Design of a nonreciprocal cloaking system. Directed optical path of (a) forward (right-to-left) propagating light and (b) backward (left-to-right) propagating light, (c) parameters for lattice resonators used for simulation, and (d) part of resonator lattice, showing 3 × 3 resonator cells with 12 intermediate coupling resonators. Actual number of resonator cells used in the entire system is far larger.

photons is not linear but is somewhat curved. This can be improved with more accurate parameter setting.

VI. Conclusion

An important requirement for practical invisibility cloaks is one-way transparency or nonreciprocity; that is, a person within the cloaked region should not be visible from the exterior but should be able to see outside the cloaking environment. To achieve such nonreciprocal cloaking, we have proposed the 'effective electromagnetic field for photons' concept, which enables us to direct light to follow a nonreciprocal path. This field can be generated using a specific photonic resonator lattice. By surrounding the cloaked region with this resonator lattice and setting the appropriate lattice parameters, we can control the transmission of light to achieve nonreciprocal cloaking. The optimal values of the lattice parameters depend on the spatial position and can be determined through the following procedure.

1. First, determine the directed optical path around the cloaked region to obtain required nonreciprocal cloaking;
2. Then, divide the space around the cloaked region into small local spaces, and determine the amplitude and direction of effective electromagnetic field for each local space to force photons to travel along the required path;
3. Finally, determine the lattice parameters (i.e., resonance frequency, $\varphi_{i(j)}$, modulation phase difference, ϕ_{ij}, and coupling strengths, V_A, V_B, and V) for every local space to create the required effective electromagnetic field.

We designed an actual cloaking system and performed ray tracing through the system with the aid of Schrödinger-equation simulation. The system successfully controlled

the travel direction of incident light to realize one-way transparency needed for nonreciprocal cloaking.

Our cloaking device, as it stands, cannot guarantee the phase matching of input and output light waves. The device can cloak amplitude images, which suffices for naked-eye spectators, but cannot cloak phase images. We are currently researching a method of cloaking both images simultaneously. We would like to discuss this on another occasion.

(It is reported that operation similar to that of the modulated resonator lattice can be achieved with moving media systems [29], [30]. This may provide another method of making nonreciprocal cloaking devices.)

REFERENCES

[1] J. B. Pendry, D. Schuring, and D. R. Smith, "Controlling electromagnetic fields," *Science*, vol. 312, no. 5781, pp. 1780–1782, May 2006.

[2] U. Leonhardt, "Optical conformal mapping," *Science*, vol. 312, no. 5781, pp. 1777–1780, May 2006.

[3] U. Leonhardt, "Notes on conformal invisibility devices," *New J. Phys.*, vol. 8, no. 7, p. 118, Jul. 2006.

[4] U. Leonhardt and T. Philbin, *Geometry and Light: The Science of Invisibility*. New York, NY, USA: Dover, 2012.

[5] R. M. Walser, "Electromagnetic metamaterials," *Proc. SPIE*, vol. 4467, pp. 1–15, Jul. 2001.

[6] S. Linden *et al.*, "Photonic metamaterials: Magnetism at optical frequencies," *IEEE J. Sel. Topics Quantum Electron.*, vol. 12, no. 6, pp. 1097–1105, Nov./Dec. 2006.

[7] S. Anantha Ramakrishna and T. M. Grzegorczyk, *Physics and Applications of Negative Refractive Index Materials*. Boca Raton, FL, USA: CRC Press, 2008.

[8] N. I. Zheldev, "A roadmap for metamaterials," *Opt. Photon. News*, vol. 22, no. 3, pp. 30–35, Mar. 2011.

[9] T. Amemiya, T. Shindo, D. Takahashi, N. Nishiyama, and S. Arai, "Magnetic interactions at optical frequencies in an InP-based waveguide device with metamaterial," *IEEE J. Quantum Electron.*, vol. 47, no. 5, pp. 736–744, May 2011.

[10] T. Amemiya, T. Shindo, D. Takahashi, S. Myoga, N. Nishiyama, and S. Arai, "Nonunity permeability in metamaterial-based GaInAsP/InP multimode interferometers," *Opt. Lett.*, vol. 36, no. 12, pp. 2327–2329, Jun. 2011.

[11] X. Ni, N. K. Emani, A. V. Kildishev, A. Boltasseva, and V. M. Shalaev, "Broadband light bending with plasmonic nanoantennas," *Science*, vol. 335, no. 6067, p. 427, Dec. 2012.

[12] D. Schurig *et al.*, "Metamaterial electromagnetic cloak at microwave frequencies," *Science*, vol. 314, no. 5801, pp. 977–980, Oct. 2006.

[13] I. I. Smolyaninov, V. N. Smolyaninova, A. V. Kildishev, and V. M. Shalaev, "Anisotropic metamaterials emulated by tapered waveguides: Application to optical cloaking," *Phys. Rev. Lett.*, vol. 102, p. 213901, May 2009.

[14] J. Valentine, J. Li, T. Zentgraf, G. Bartal, and X. Zhang, "An optical cloak made of dielectrics," *Nature Mater.*, vol. 8, no. 7, pp. 568–571, Apr. 2009.

[15] A. J. Danner, "Visualizing invisibility: Metamaterials-based optical devices in natural environments," *Opt. Exp.*, vol. 18, no. 4, pp. 3332–3337, Feb. 2010.

[16] M. Gharghi *et al.*, "A carpet cloak for visible light," *Nano Lett.*, vol. 11, no. 7, pp. 2825–2828, May 2011.

[17] X. Zang, B. Cai, and Y. Zhu, "Shifting media for carpet cloaks, antiobject independent illusion optics, and a restoring device," *Appl. Opt.*, vol. 52, no. 9, pp. 1832–1837, Mar. 2013.

[18] K. Fang, Z. Yu, and S. Fan, "Realizing effective magnetic field for photons by controlling the phase of dynamic modulation," *Nature Photon.*, vol. 6, no. 11, pp. 782–787, Oct. 2012.

[19] K. Fang and S. Fan, "Effective magnetic field for photons based on the magneto-optical effect," *Phys. Rev. A*, vol. 88, p. 043847, Oct. 2013.

[20] J. M. Luttinger, "The effect of a magnetic field on electrons in a periodic potential," *Phys. Rev.*, vol. 84, no. 4, pp. 814–817, Nov. 1951.

[21] R. O. Umucallar and I. Carusotto, "Artificial gauge field for photons in coupled cavity arrays," *Phys. Rev. A*, vol. 84, no. 4, p. 043804, Oct. 2011.

[22] M. Graf and P. Vogl, "Electromagnetic fields and dielectric response in empirical tight-binding theory," *Phys. Rev. B*, vol. 51, no. 8, pp. 4940–4949, Feb. 1995.

[23] R. Peierls, "Zur theorie des diamagnetismus von leitungselektronen," *Zeitschrift Phys.*, vol. 80, nos. 11–12, pp. 763–791, 1933.

[24] T. J. Kippenberg and K. J. Vahala, "Cavity opto-mechanics," *Opt. Exp.*, vol. 15, no. 25, pp. 17172–17205, Dec. 2007.

[25] T. J. Kippenberg and K. J. Vahala, "Cavity optomechanics: Back-action at the mesoscale," *Science*, vol. 321, no. 5893, pp. 1172–1176, Aug. 2008.

[26] W. Shimizu, N. Naomi, K. Kohno, K. Hirakawa, and M. Nomura, "Waveguide coupled air-slot photonic crystal nanocavity for optomechanics," *Opt. Exp.*, vol. 21, no. 19, pp. 21961–21969, Sep. 2013.

[27] J. Chan *et al.*, "Laser cooling of a nanomechanical oscillator into its quantum ground state," *Nature*, vol. 478, no. 7367, pp. 89–92, Oct. 2011.

[28] J. N. Winn, S. Fan, J. D. Joannopoulos, and E. P. Ippen, "Interband transitions in photonic crystals," *Phys. Rev. B*, vol. 59, no. 3, pp. 1551–1554, Jan. 1999.

[29] U. Leonhardt and P. Piwnicki, "Optics of nonuniformly moving media," *Phys. Rev. A*, vol. 60, no. 6, pp. 4301–4312, Dec. 1999.

[30] T. G. Philbin, C. Kuklewicz, S. Robertson, S. Hill, F. König, and U. Leonhardt, "Fiber-optical analog of the event horizon," *Science*, vol. 319, no. 5868, pp. 1367–1370, Mar. 2008.

Tomohiro Amemiya (S'06–M'09) received the B.S. and Ph.D. degrees in electronics engineering from the University of Tokyo, Tokyo, Japan, in 2004 and 2009, respectively.

He joined the Quantum Electronics Research Center, Tokyo Institute of Technology, Tokyo, in 2009, where he is currently an Assistant Professor. Since 2014, he has been a Visiting Fellow with RIKEN, Tokyo.

His research interests include the physics of semiconductor light-controlling devices, metamaterials for optical frequencies, magneto-optical devices, and the technologies for fabricating these devices.

Dr. Amemiya is a member of the Optical Society of America, the American Physical Society, and the Japan Society of Applied Physics. He was a recipient of the 2007 IEEE Photonics Society Annual Student Paper Award, the 2008 IEEE Photonics Society Graduate Student Fellowship, and the 2012 Konica Minolta Imaging Award.

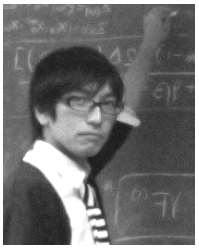

Masato Taki received the B.S. and Ph.D. degrees in physics from the University of Tokyo, Tokyo, Japan, in 2004 and 2009, respectively.

He was a Post-Doctoral Fellow with the Yukawa Institute for Theoretical Physics, Kyoto University, Kyoto, Japan, from 2009 to 2013. In 2013, he joined the RIKEN Nishina Center for Accelerator-Based Science, Wako, Japan, where he is currently a Senior Research Scientist.

His research interests lie in string theory, gauge theory, and mathematical physics. He is currently studying the 5-D N=1 supersymmetric gauge theory by employing the relation between topological string and M/F-theory, and also studying the newly discovered duality between 4-D gauge theories and 2-D conformal field theories, which is called the AGT correspondence.

Dr. Taki is a member of the American Physical Society and the Physical Society of Japan.

Toru Kanazawa (M'09) received the B.S. and Ph.D. degrees in electronics and applied physics from the Tokyo Institute of Technology, Tokyo, Japan, in 2002 and 2007, respectively.

He joined the Department of Physical Electronics, Tokyo Institute of Technology, Tokyo, in 2007, where he is currently an Assistant Professor.

His research interests include the physics of III–V-based transistors and the technologies for fabricating these devices.

Dr. Kanazawa is a member of the Japan Society of Applied Physics.

Takuo Hiratani (S'13) received the B.E. degree in electrical and electronic engineering from Kanazawa University, Ishikawa, Japan. He is currently pursuing the Ph.D. degree in electrical and electronic engineering with the Tokyo Institute of Technology, Tokyo, Japan.

His current research interests include membrane-based photonic devices for optical interconnection.

Mr. Hiratani is a Student Member of the Institute of Electronics, Information and Communication Engineers, and the Japan Society of Applied Physics.

Shigehisa Arai (M'83–SM'06–F'10) is currently a Professor with the Quantum Nanoelectronics Research Center, Tokyo Institute of Technology, Tokyo, Japan, where he is also with the Department of Electrical and Electronic Engineering. He received the B.E., M.E., and D.E. degrees in electronics engineering from the Tokyo Institute of Technology, in 1977, 1979, and 1982, respectively.

He joined the Department of Physical Electronics, Tokyo Institute of Technology, as an Assistant Professor, in 1982, where he became an Associate Professor in 1987, and a Professor with the Research Center for Quantum Effect Electronics in 1994. Since 2004, he has been a Professor with the Quantum Nanoelectronics Research Center, Tokyo Institute of Technology. From 1983 to 1984, he was with AT&T Bell Laboratories, Holmdel, NJ, USA. His research interests include photonic integrated devices, such as dynamic-single-mode and wavelength-tunable semiconductor lasers, semiconductor optical amplifiers, and optical switches/modulators, and studies on low-damage and cost-effective processing technologies of ultrafine structures for high-performance lasers and photonic integrated circuits on silicon platforms.

Dr. Arai is a member of the Optical Society of America, the Institute of Electronics, Information and Communication Engineers (IEICE), and the Japan Society of Applied Physics. He was a recipient of the Excellent Paper Award from the IEICE of Japan in 1988, the Michael Lunn Memorial Award from the Indium Phosphide and Related Materials Conference in 2000, and the Prizes for Science and Technology, including the Commendation for Science and Technology from the Minister of Education, Culture, Sports, Science and Technology in 2008, the Electronics Society Award from IEICE in 2008, and the JSAP Fellowship in 2008.